Published in final edited form as:
Mol Imaging. 2006 ; 5(1): 31–40.

Imaging Molecular Expression on Vascular Endothelial Cells by In Vivo Immunofluorescence Microscopy

Judith M. Runnels[*], **Parisa Zamiri**[*], **Joel A. Spencer**[*], **Isreal Veilleux**[*], **Xunbin Wei**[*], **Alexei Bogdanov**[†], and **Charles P. Lin**[*]
Massachusetts General Hospital, USA

Abstract

Molecular expression on the vascular endothelium is critical in regulating the Interaction of circulating cells with the blood vessel wall. Leukocytes as well as circulating cancer cells gain entry into tissue by interacting with adhesion molecules on the endothelial cells (EC). Molecular targets on the EC arc increasingly being explored for tissue-specific delivery of therapeutic and Imaging agents. Here we use in vivo immunofluorescence microscopy to visualize the endothelial molecular expression in the vasculature of live animals. High-resolution images are obtained by optical sectioning through the intact skin using in vivo confocal and multiphoton microscopy after in situ labeling of EC surface markers with fluorescent antibodies. Other vascular beds such as the bone marrow and ocular blood vessels can be imaged with little or no tissue manipulation. Live imaging is particularly useful for following the dynamic expression of inducible molecules such as E-selectin during an inflammatory response.

Keywords

Imaging; in vivo confocal microscopy; multiphoton microscopy; adhesion molecules; selectins

Introduction

The vascular endothelium is a single cell lining of blood vessels that is intimately involved in the regulation of cellular and molecular transport between blood and tissue compartments. As such, it plays an active role in such diverse processes as cell migration during development [1,2], inflammation [3], leukocyte homing [4], and metastasis (5). These processes are governed by the endothelial cells (EC) through the expression of chemokines and adhesion molecules on the cell surfaces. Among the adhesion molecules contributing to these functions are the integrins, the immunoglobulin superfamily, and the selectins [6]. Leukocyte migration to sites of tissue injury or inflammation, for example, begins with selectin-mediated tethering and rolling along the vascular wall [7–10] followed by integrin-mediated adhesion and platelet endothelial cell adhesion molecule (PECAM-1)-mediated transmigration [11–13]. Vascular adhesion markers are often upregulated in disease and can contribute to the disease process [14,15]. Therapeutic measures directed against adhesion molecules can attenuate disease processes [16], and expression of adhesion molecules can serve as treatment monitors. For these reasons, a real-time in vivo system that can detect adhesion molecules, monitor their expression, and enable biological processes to be followed within individual animals is desirable.

Corresponding author: Charles P. Lin, Wellman Center for Photomedicine, BHX 630. Massachusetts General Hospital, 55 Fruit Street, Boston. MA 02114; Lin@helix.mgh.harvard.edu.
[*]Advanced Microscopy Program, Wellman Center for Photobiology
[†]Center for Molecular Imaging Research

Detailed understanding of the mechanisms governing leukocyte recruitment has emerged with the aid of intravital microscopy [16], a powerful method that enables real-time observation of leukocyte rolling, adhesion, and transendothelial migration in vivo [18–25] as well as platelet interactions with the vasculature [26].

One shortcoming of the standard intravital microscopy technique is the inability to visualize the participation of the EC in the leukocyte recruitment process. Here we describe the use of in vivo immunofluorescence microscopy for direct visualization of mouse vascular EC. Specifically, we image molecular expression on the vascular EC after intravenous introduction of fluorescent antibodies against EC surface markers. Binding of the antibodies over time is imaged noninvasively using in vivo confocal and multiphoton microscopy, which allows optical sectioning through the intact skin of live animals. This system is useful for studying individual cell populations in situ over time, which are involved in dynamic processes and identifiable by specific cell surface markers. Normal and disease processes can be followed over long periods in individual animals.

Materials and Methods

Animals

All mice were maintained according to the policies of the Massachusetts General Hospital Subcommittee on Research Animal Care of the Institutional Animal Care and Use Committee. Young healthy female Balb/c mice were obtained from Charles River Laboratories (Wilmington, MA). E-selectin knockout mice derived in a Balb/c background were the kind gift of Dr. David Milstone, Harvard Medical School. Anesthesia was accomplished by intramuscular injection of ketamine/xylazine. Ocular imaging was done on young C57B16 mice from Charles River Laboratories.

Antibody Conjugations

Monoclonal antibodies (mAbs) directed against mouse PECAM-1 (FITC-conjugated and purified rat anti-mouse CD31-clone MEC 13.3), mouse E-selectin (rat anti-mouse CD62E-clone 10E9.6), P-selectin (rat anti-mouse CD62P-clone RB40.34), and vascular adhesion molecule (VCAM)-l (rat anti-mouse CD106 clone 429[MVCAM.A]) antibodies were obtained from BD Biosciences/Pharmingen (San Diego, CA). Cy5.5 was obtained from Amersham Pharmacia (Piscataway, NJ), and IRDye 38 was the kind gift of Mr. Harry L. Osterman of LI-COR Corp (Lincoln, NE). Antibodies were conjugated to the respective dyes using the manufacturers' recommended protocols. Cy5.5 and IR38 dyes were conjugated to antibodies in ratios of two to four dye molecules per protein molecule. The quantum yield of Cy5.5 is greater than 0.28 for a conjugate with a dye-to-protein ratio of 2. The chemical structure of IRDye 38 is shown below in Figure 1:

Confocal/Two-Photon Microscope

This system is built on a video-rate scanning laser confocal microscope platform previously developed in this laboratory for real-time noninvasive imaging of human skin [27,28], modified to include a femtosecond Ti:sapphire laser (Coherent Mira, Santa Clara, CA) for two-photon excitation of FITC-conjugated antibodies. The same Ti:sapphire laser, tuned to 760 nm, was used for one-photon excitation of IRDye 38. Antibodies conjugated to Cy5.5 were excited with either a helium-neon laser at 633 nm or a diode laser (Micro Laser Systems, Garden Grove, CA) at 656 nm. Two separate photomultiplier tubes (Hamamatsu, Bridgewater, NJ) are each optimized for one-photon detection (descanned channel with confocal aperture) and two-photon detection (nondescanned channel with no confocal aperture). The system operates at a user-selectable frame rate from 15 to 30 fps. High-resolution images with cellular details are obtained through the intact mouse skin at depths

of up to 150 μm from the surface of the skin, using a 30 × 0.9NA (LOMO Optics, Prospect Heights, IL) or a 60X 1.2NA (Olympus, Melville, NY) water-immersion objective lens. This depth is sufficient for imaging most of the dermal vasculature.

In Vivo Imaging

Mice were anesthetized, and injected with fluorescently conjugated antibody via the tail vein using 30 G needles. Cy5.5 anti-E-selectin, Cy5.5 anti-P-selectin, and IRDye 38 anti-E-selectin were used at the concentration of 0.5 mg/kg (10–12 μg/mouse) and Cy5.5-conjugated VCAM-1 or FITC-conjugated anti-PECAM was injected at 1.0 mg/kg (20–24 μg/mouse). All antibodies were diluted with Dulbecco's phosphate-buffered saline (DPBS, Mediatech, Inc., Herndon, VA) and injected in a 200- to 250-μl volume. Animals were placed on a warmed microscope stage or in a 50-ml conical tube (Falcon, Division of BD Biosciences, Bedford, MA) fitted with a heating coil.

Induced E-selectin Expression

Constitutive skin E-selectin expression was visualized by injection of Cy5.5-conjugated anti-mouse CD62E followed by IR38-conjugated anti-mouse CD62E 9 days later. At that time, E-selectin expression was induced by intraperitoneal injection of 50 μg *E. coli* lipopolysaccharide (LPS, Sigma, St. Louis, MO) in 50 μl saline.

To demonstrate E-selectin induction in conjunctiva, animals received Cy5.5-conjugated anti-E-selectin antibody and were imaged 24 hr later. The same mice then received systemic LPS together with intravenous IRDye 38-conjugated E-selectin. The effect of LPS on E-selectin expression in the conjunctiva was measured 24 hr later by in vivo confocal microscopy.

Ocular Imaging

Following anesthesia, the pupil was dilated with 1% tropicanide, and a coverslip was placed over the corneal surface moistened with the 2% methylcellulose. The retina was imaged using a 20 × 0.42NA long-working-distance objective lens (Mitutoyo, Aurora, IL). For choroidal and conjunctival images, a 10-O suture was placed at the temporal aspect of the limbus, and the temporal conjunctiva was gently released using microscissors. The eye was rotated nasally using the suture ends to expose the conjunctiva and choroid. The cover-slip was placed on the exposed area with the aid of 2% methylcellulose, and the conjunctiva and choroid were visualized using in vivo confocal microscopy. To demonstrate the changes in VCAM-1 expression in the retinal vasculature, Cy5.5-conjugated anti-VCAM-1 antibody was injected intravenously into control and mice subjected to systemic LPS treatment 24 hours earlier.

Results

Optical Sectioning Minimizes Tissue Autofluorescence Background

In these studies we have used a custom-built confocal/two-photon microscope that is optimized for small animal imaging and for detecting the weak immunofluorescence signal in the presence of the stronger tissue autofluorescence background. For both one-photon and two-photon fluorescence excitation, the laser beam is focused to a small focal spot (~1 × 1 × 5 μm [27,28]) and raster scanned to obtain a two-dimensional image called an optical section. Images can be acquired at up to 30 frames per second (video rate), whereas successive optical sections can be obtained by focusing at different depths into tissue. For confocal microscopy, optical sectioning is achieved by placing a confocal pinhole in front of the detector to reject out of focus photons. The signal photons, coming from the in-focus plane in a raster-scanned fashion, need to be "descanned" in order to pass through the stationary confocal pinhole. In contrast, two-photon fluorescence is induced only at the

focus of the mode-locked (femtosecond) laser pulses where sufficient intensity is reached for the nonlinear excitation. Optical sectioning is obtained automatically from the focal plane without the need for a confocal pinhole, hence without the need for descanning. A separate photomultiplier is used in the "non-descanned" position for detecting the two-photon fluorescence signal. We use a near-infrared laser source (Ti:sapphire laser running at 800 nm) to excite FITC-conjugated antibodies (excitation maximum = 494 nm, emission maximum = 530 nm). As is well known, two-photon excitation at 800 nm allows deeper imaging into tissue compared to one-photon excitation of the same fluorophore at 488 nm. However, when we compare two-photon excitation of FITC and one-photon excitation of Cy5.5-conjugated antibodies (excited with a HeNe laser at 633 nm and detected at 694 nm), we obtained comparable tissue penetration depths (~150 μm in the mouse skin). Figure 2 shows different optical sections from the mouse skin, excited at 633 nm, with prominent autofluorescence features coming from the hair (Figure 2A) and the epidermis (Figure 2B). Dermal vasculature, labeled with Cy5.5-conjugated antibody against the ubiquitous endothelial cell surface marker CD31 (PECAM-1), is detected in deeper optical sections, approximately 50–100 μm below the skin surface (Figure 2C). Autofluorescence from the hair follicles and the sebaceous glands can also be detected at these depths. With an injected dose of 0.5–1 μg/g of body weight (10–20 μg per mouse) the optimal time for imaging the endothelial labeling is typically 16–24 hr after antibody injection because the unbound mAb is mostly cleared from the circulation by this time (Figure 2C). The animal appears to tolerate this mAb concentration well with no obvious adverse effects. PECAM-1 endothelial labeling remains visible for 3–4 days after a single injection. Nonspecific isotype control IgG shows no detectable binding to the EC (figure not shown).

Tissue Autofluorescence Background Decreases with Increasing Wavelength

Figure 3 shows the relative level of the labeled endothelial signal to the skin autofluorescence background for three different fluorophores with increasing wavelengths: FITC (excitation maximum = 494 nm, emission maximum = 530 nm, Figure 3A and B), Cy5.5 (excitation maximum = 678 nm, emission maximum = 694 nm, Figure 3C–E), and IR38 (excitation maximum = 778 nm, emission maximum = 806 nm, Figure 3F and G). As expected, the shortest wavelength channel has the highest autofluorescence background, which limits the detection sensitivity of the current method. The detection sensitivity can be determined by injecting successively lower doses of control IgG molecules into the circulation and measuring the signal-to-background ratio using fluorescence intensities in the plasma (signal) and in the extravascular tissue (background), respectively. With 3 μg of circulating antibody (0.15 μg/g of body weight) optimally labeled with Cy5.5 at a dye/protein ratio of 2–4, we obtained a signal-to-background ratio of 2:1. Taking the total blood volume to be ~2 mL per mouse, the minimum detectable antibody concentration can be estimated to be 10 nM. Assuming a voxel volume of ~5 fL (1 × 1 × 5 μm), the minimum number of antibody molecules that can be detected in each voxel is 30.

Simultaneous Confocal Immunofluorescence Imaging Reveals Distinct Expression Patterns of PECAM-1, E-selectin, and P-selectin in Quiescent Skin

Coexpression of two or more endothelial cell markers can be visualized by labeling them with different fluorescent probes and imaging with a combination of confocal (one-photon fluorescence) and two-photon fluorescence microscopy. Colocalizations of PECAM-1 and E-selectin as well as E-selectin and P-selectin in the cutaneous vascular lumen are shown in Figures 4 and 5, respectively. Colocalization of PECAM-1 and E-selectin (Figure 4C) was obtained by in vivo double labeling with anti-PECAM-1 (FITC) (Figure 4A and D) and anti-E-selectin (Cy5.5) (Figure 4B and E) antibodies. The green channel shown in Figure 4A and D is obtained by two-photon excitation of FITC-anti-PECAM-1 mAb using a Ti:Al_2O_3 laser at 800 nm, whereas the red channel (Figure 4B, E) is obtained by one-photon excitation of

Cy5.5-anti-E-selectin mAb using a HeNe laser at 633 nm. As seen in the image overlay (Figure 4C), E-selectin colocalizes with a subset of blood vessels that stain positive for PECAM-1. In addition, Figure 4D and E demonstrates that E-selectin mAb labels only small vessels, whereas PECAM-1 mAb is bound to those small vessels as well as larger ones. By observing real-time images acquired at video rate, we can identify the vessels that express E-selectin as postcapillary venules based on size and the direction and speed of flow of low-level, unbound fluorescent mAb in the blood stream. E-selectin is absent in the arterioles or the capillaries, as well as larger veins (>50 μm diameter), whereas PECAM-1 is expressed on all vessels. Although the PECAM-1 labeling slowly fades away in 3–4 days, vessels that stain positive for E-selectin retain their fluorescence for up to 2 weeks. We attribute the slow accumulation and persistent staining to internalization of the anti-E-selectin probe because it is known that endothelial E-selectin is internalized very efficiently into multivesicular bodies [29–31]. In contrast, PECAM-1 is poorly internalized [32]. Consistent with these observations, the E-selectin staining pattern on the vessel wall often has a discrete, granular appearance in contrast to the more uniform distribution of the PECAM-1 probe. The latter probably reflects extended retention of PECAM-1 on the cell surface.

In vivo double labeling of E-selectin and P-selectin reveals a distinct staining pattern for the two selectins (Figure 5), which has not been described previously. Whereas E-selectin expression is restricted to small (< 50 μm) postcapillary venules (Figure 5A, B), P-selectin is expressed in both small (< 50 μm) and larger (> 50 μm) venules (Figure 5C, D). P-selectin staining also shows a granular appearance, consistent with efficient endocytosis of P-selectin [33] to either Weibel-Palade bodies [29] or lysosomes.

E-selectin Knockout Mice Demonstrate Specificity of In Vivo Antibody Labeling

In order to verily that cutaneous E-selectin labeling in vivo reflects true constitutive expression of this adhesion molecule rather than nonspecific binding, the 10E9.6 monoclonal antibody (anti-CD62E) was tested against anti-CD62P antibody using E-selectin knockout mice. Labeling with Cy5.5–anti-E- and P-selectins reveals that P-selectin is expressed in the venules of both the control (Figure 6D) and the E-selectin knockout mice (Figure 6B), whereas E-selectin is detected only in the vessels of wild-type mice (Figure 6A vs. C).

LPS Induces E-selectin Expression on Large Vessels in Skin

E-selectin is a well-known inducible marker of inflammation. To determine if we could detect differences in constitutive and induced E-selectin expression in vivo, we used anti-E-selectin antibody conjugated to two different fluorophores, Cy5.5 and IRDye38. The Cy5.5-conjugated probe was first injected intravenously into a normal BALB/c mouse to measure baseline expression. Subsequently, 50 μg of LPS was administered intraperitoneally to induce systemic inflammation [33], and the IRDye38-conjugated probe was injected intravenously to measure the expression during the inflammatory response. Images were taken 3 days following the second injection. Because the EC retain the E-selectin probes, both Cy5.5 and IRDye38 probes are visible at the time of imaging. As in earlier experiments, E-selectin was expressed constitutively in the postcapillary venules of the mouse ear as shown in the Cy5.5 channel (Figure 7A). The lRDye38 image (Figure 7B), however, shows that the LPS-induced E-selectin was found not only in the postcapillary venules, but over greater segments of the venous vasculature including larger veins (>50 μm).

Application of In Vivo Immunofluorescence Microscopy to Image EC Surface Marker Expression in Other Tissues

Tissues of the eye are susceptible to conditions that alter adhesion molecule expression, which can result in severe consequences. Adhesion molecules are upregulated in various ocular inflammatory and angiogenic conditions, such as diabetes and uveitis [14,34] and age-related macular degeneration [35]. For this reason, direct observation of adhesion molecule expression in the eyes of living organisms is desirable. We have previously demonstrated that in vivo immunofluorescence microscopy can be applied to vascular beds other than skin with little (e.g., bone marrow [36]) manipulation. Here we show that visualization of various vascular beds in the murine eye is also possible with little or no manipulation (Figure 8). Using a coverslip placed on the corneal surface and a 20 × 0.42NA long-working-distance objective lens, PECAM-1 expression is demonstrated in all vascular compartments of the retina, including the capillaries (Figure 8A). Similarly, PECAM-1 expression is noted in the choroid of the eye (Figure 8B), where upregulation of adhesion molecules has been seen in the context of age-related macular degeneration [35].

To demonstrate changes in VCAM-1 expression in the retinal vasculature, anti-VCAM-1 antibody conjugated to Cy5.5 fluorophore was injected intravenously into the tail vein of mice 24 hr after systemic administration of LPS (Figure 8D) and in control mice (Figure 8C). Upregulation of VCAM-1 expression is clearly demonstrated in the LPS-treated animal (Figure 8C and D). Upregulation of E-selectin is also demonstrated in the conjunctiva of the eye (Figure 8E and F). In this case, mice were first injected intravenously with Cy5.5-conjugated anti-E-selectin antibody (Day 0). Twenty-four hours later (Day 1), the mice were imaged, and constitutive E-selectin expression was observed in the conjunctiva. LPS was then administered systemically to the same animals, together with IR-conjugated anti-E-selectin mAb, and on Day 2, the animals were imaged again using both fluorescence channels. As it is clearly demonstrated in Figure 8, E-selectin is expressed constitutively in the conjunctival vessels, but its expression is significantly increased after administration of the inflammatory agent, LPS (Figure 8E and F).

Discussion and Conclusions

Leukocyte-endothelial interactions are dependent on molecular signals displayed on the EC surfaces. As the immune response is a dynamic process, the molecular signals are expressed in a spatially as well as temporally specific manner [37]. Traditional methods such as immunohistochemistry require tissue extraction/processing and provide only snapshots of endothelial expression at single time points. In addition, immunohistochemical methods yield little three-dimensional information because tissue is cut into thin sections. Intravital microscopy has proved to be a powerful method for visualizing leukocyte trafficking in vivo and has led to a wealth of new understanding on how circulating cells home to different tissue sites under normal and diseased conditions. However, endothelial molecular expression is usually not directly visualized in these studies. Instead, the contributions of specific cell adhesion molecules to the leukocyte-endothelial interaction are determined indirectly by comparing the leukocyte trafficking patterns before and after treatment with an interfering antibody or peptide directed against the adhesion molecules [18–20], or by comparing wild-type and knockout animals [38]. Although these functional studies are essential, they do not reveal the detailed spatial distribution of the molecules under investigation. Newer methods image molecular expression in vivo by labeling endothelial cell markers with immunoconjugates of magnetic resonance [39,40], ultrasound [41], or radionuclide contrast agents [33,42], but these methods lack the spatial resolution to visualize single cells and small blood vessels.

Here we demonstrate that the temporal and spatial relationships of vascular endothelium molecular expression can be visualized directly using the method of in vivo immunofluorescence microscopy. Through optical sectioning, this method provides three-dimensional information on the architecture of the vasculature, and because it is noninvasive in nature, the same animals can be imaged repeatedly to yield temporal data. Endothelial cell surface molecules are labeled with fluorescent antibodies injected into the circulation, and the vasculature of the skin or the eye can be imaged noninvasively in live animals over time. Other vascular beds, as in bone marrow [36], can be imaged with minimum tissue manipulation. We have used primary antibody concentrations of 0.5–1.0 mg/kg, which does not appear to be saturating because the fluorescence signal increases with increasing antibody dosage (data not shown). In addition, we have shown in another work [36] that leukemic and progenitor/stem cell homing and engraftment to bone marrow vasculature are not affected by the presence of antibodies against E-selectin and SDF-1 at similar concentrations, indicating minimal perturbation to cell function. Falati et al. [26] demonstrated the formation of thrombii in the presence of primary antibody concentrations nearly 10 times higher than used in the current work.

The use of optical sectioning techniques such as confocal or multiphoton microscopy greatly enhances the capacity to detect the weak immunofluorescence signal amid the stronger tissue autofluorescence background. Imaging depth is limited by tissue scattering to about 150 μm in the skin, but this depth is sufficient for visualizing most of the vascular structures in the mouse skin as well as the marrow of the flat bone of the skull. In addition, the fast image-acquisition speed (up to video rate at 30 frames per second) allows us to image moving targets such as rolling leukocytes as in standard intravital microscopy [43]. For stationary targets, such as endothelial cells, the imaging speed makes it possible to survey relatively large tissue volumes (e.g., most of the mouse ear).

Using this method, we are able to detect (1) PECAM-1 expression in the vasculature of skin, retina, and choroid; (2) E-selectin constitutive expression in the small postcapillary venules with diameters less than 50 μm in normal mouse skin and upregulation in large venules (>50 μm) in skin after LPS treatment; (3) upregulation of E-selectin in conjunctiva after LPS induction; and (4) P-selectin constitutive expression in normal mouse skin both in small (<50 μm) and larger (>50 μm) venules.

Our results agree with the finding that E-selectin is expressed in the skin of the mouse under normal, non-inflammatory conditions. In addition, in vivo immunufluorescence confocal microscopy revealed that E-selectin in skin is expressed in venules of varying sizes in the quiescent and induced states, with constitutively expressed E-selectin restricted to small postcapillary venules. The data presented here are consistent with the argument that E-selectin expression in the skin may be specifically designed to enable memory T cells expressing cutaneous lymphocyte antigen (CLA) to roll slowly and perform immune surveillance [44]. P-selectin expression in normal skin is also restricted to the venules, but in contrast to E-selectin is found in both small and large venules. The pattern of EC molecular expression controls the nature of an immune response at a given site [45–47]. Antibody blocking studies using in vivo fluorescence microscopy may be used to dissect these relationships.

In summary, this article demonstrates the use of in vivo immunofluorescence microscopy to directly characterize EC surface marker expression in mouse skin and eye under normal and inflamed conditions. The major advantage of the live imaging approach is that (1) spatial and temporal relationships in the expression of individual cell markers can be determined using multichannel imaging; (2) as a result, the three dimensional architecture of the vasculature can be discerned, and specific cell populations can be dynamically followed; and

(3) individual experimental animals can be imaged repetitively over several days or weeks to follow the time course of disease progression or response to therapy. This method will be particularly useful for studying processes such as inflammation, angiogenesis, atherogenesis, and diabetic retinopathy, which are closely associated with EC activation, proliferation, or dysfunction.

Acknowledgments

This work was supported by NIH grants EB000664 and EY14106. We thank Alan Prossin, MD, for assistance in animal dissection, and Suzanne Harvey for able help with the manuscript and figures. IR38 dye was the gift of Harry Osterman (LI-COR Corp.)

Abbreviations

CD31	PECAM-1 (platelet-endothelial cell adhesion molecule)
CD62E	E-selectin
CD62P	P-selectin
EC	endothelial cell
FITC	fluorescein isothiocyanate
LPS	lipopolysaccharide
mAb	monoclonal antibody
VCAM-1	vascular cell adhesion molecule-1

References

1. Hynes RO. Integrins, versatility, modulation, and signalling in cell adhesion. Cell. 1992; 69:11–25. [PubMed: 1555235]
2. Rouslahti E. Extracellular matrix/growth factor interactions. Cold Spring Harb Symp Quant Biol. 1992; 57:309–315. [PubMed: 1339667]
3. Bullard DC, Kunkel EJ, Kubo H, Hicks MJ, Lorenzo I, Doyle NA, Doerschuk CM, Ley K, Beaudet AL. Infectious susceptibility and severe deficiency of leukocyte rolling and recruitment in E-selectin and P-selectin double mutant mice. J Exp Med. 1996; 183:2329–2396. [PubMed: 8642341]
4. Schweitzer KM, Drager AM, van der Valk P, Thijsen SFT, Zevenbergen A, Theijsmeijer AP, van der Schoot CE, Langenhuisen MMAC. Constitutive expression of E-selectin and vascular cell adhesion molecule-1 on endothelial cells of hematopoietic tissues. Am J Pathol. 1996; 148:165–175. [PubMed: 8546203]
5. Rice GE, Bevilacqua MP. An inducible endothelial cell surface glycoprotein mediates melanoma adhesion. Science. 1989; 24:1303–1306. [PubMed: 2588007]
6. Panes J, Perry M, Granger DN. Leukocyte-endothelial cell adhesion: Avenues for therapeutic intervention. Br J Pharmacol. 1999; 126:537–550. [PubMed: 10188959]
7. Lasky LA. Selectin-carbohydrate interactions and the initiation of the inflammatory response. Annu Rev Biochem. 1995; 64:113–139. [PubMed: 7574477]
8. Vestweber D, Blanks JE. Mechanisms that regulate the function of the selectins and their ligands. Physiol Rev. 1999; 79:181–213. [PubMed: 9922371]
9. Springer TA. Traffic signals for lymphocyte recirculation and leukocyte emigration: The multistep paradigm. Cell. 1994; 76:301–314. [PubMed: 7507411]
10. McEver RP, Cummings RD. Role of PSGL-1binding to selectins in leukocyte recruitment. J Clin Invest. 1997; 100:485–491. [PubMed: 9239393]
11. Kulidjian AA, Inman R, Issekutz TB. Rodent models of lymphocyte migration. Semin Immunol. 1999; 11:85–93. [PubMed: 10329495]

12. Carlos TM, Harlan JM. Leukocyte-endothelial adhesion molecules. Blood. 1994; 84:2068–2101. [PubMed: 7522621]
13. Muller WA, Randolph GJ. Migration of leukocytes across endothelium and beyond: Molecules involved in the transmigration and fate of monocytes. J Leukoc Biol. 1999; 66:698–704. [PubMed: 10577496]
14. Joussen AM, Poulaku V, Le ML, Koizumi K, Esser C, Janicki H, Schraermeyer U, Kociok N, Fauser S, Kirchof B, Kern TS, Adamis AP. A central role for inflammation in the pathogenesis of diabetic retinopathy. FASEB J. 2004; 18:1450–1452. [PubMed: 15231732]
15. Ley K. The role of selectins in inflammation and disease. Trends Mol Med. 2003; 9:263–268. [PubMed: 12829015]
16. Miyamoto K, Khosrof S, Bursell S-E, Rohan R, Murata T, Clermont AC, Aiello LP, Ogura Y, Adamis AP. Prevention of leukostasis and vascular leakage in streptozotocin-induced diabetic retinopathy via intercellular adhesion molecule-1 inhibition. Proc Natl Acad Sci USA. 1999; 96:10836–10841. [PubMed: 10485912]
17. Mempel T, Scimoni ML, Mora JR, von Andrian UH. In vivo imaging of leukocyte trafficking in blood vessels and tissues. Curr Opin Immun. 2004; 16:406–417.
18. Eriksson EE, Werr J, Guo Y, Thoren P, Lindbom L. Direct observation in vivo on the role of endothelial selectins and α4 integrin in cytokine-induced leukocyte-endothelium interactions in the mouse aorta. Circ Res. 2000; 86:526–533. [PubMed: 10720414]
19. Robert C, Fuhlbrigge RC, Kieffer JD, Avehunie S, Hynes RO, Cheng G, Grabbe S, von Andrian UH, Kupper TS. Interaction of dendritic cells with skin endothelium: A new perspective on immunosurveillance. J Exp Med. 1999; 189:627–635. [PubMed: 9989977]
20. oude Egbrink MGA, Janssen GHGW, Ookawa K, Slaaf DW, Reneman RS, Wehrens XHT, Maaijwee KJM, Ohshima N, Struijker Boudier HAJ, Tangelder GJ. Especially polymorphonuclear leukocytes, but also monomorphonuclear leukocytes, roll spontaneously in venules of intact rat skin: Involvement of E-selectin. J Invest Dermatol. 2002; 118:323–326. [PubMed: 11841551]
21. Warnock RA, Askari S, Butcher EC, von Andrian UH. Molecular mechanisms of lymphocyte homing to peripheral lymph nodes. J Exp Med. 1998; 187:205–216. [PubMed: 9432978]
22. Bargatze RF, Jutila MA, Butcher EC. Distinct roles of L-selectin and integrins α4β7 and LFA-1 in lymphocyte homing to Peyer's patch-HEV in situ: The multistep model confirmed and refined. Immunity. 1995; 3:99–108. [PubMed: 7542550]
23. Stein JV, Rot A, Luo Y, Narasimhaswamy M, Nakano H, Gunn MD, Matsuzawa A, Quackenbush EJ, Dorf ME, von Andrian UH. The CC chemokine thymus-derived chemotactic agent 4 (TCA-4, secondary lymphoid tissue chemokine, 6Ckine, exodus-2) triggers lymphocyte function-associated antigen 1-mediated arrest of rolling T lymphocytes in peripheral lymph node high endothelial venules. J Exp Med. 2000; 191:61–76. [PubMed: 10620605]
24. Warnock RA, Campbell JJ, Dorf ME, Matsuzawa A, McEvoy LM, Butcher EC. The role of chemokines in the microenvironmental control of T versus B cell arrest in Peyer's patch high endothelial venules. J Exp Med. 2000; 191:77–88. [PubMed: 10620606]
25. Okada T, Ngo VN, Ekland EH, Forster R, Lipp M, Littman DR, Cyster JG. Chemokine requirements for B cell entry to lymph nodes and Peyer's patches. J Exp Med. 2002; 196:65–75. [PubMed: 12093871]
26. Falati S, Gross P, Merrill-Skoloff G, Furie BC, Furie B. Real-time in vivo imaging of platelets, tissue factor, and fibrin during arterial thrombus formation in the mouse. Nat Med. 2002; 8:1175–1181. [PubMed: 12244306]
27. Rajadhyaksha M, Grossman M, Esterowitz D, Webb RH, Anderson RR. In vivo confocal scanning laser microscopy of human skin: Melanin provides strong contrast. J Invest Dermatol. 1995; 104:946–952. [PubMed: 7769264]
28. Rajadhyaksha M, Gonzalez S, Zavislan JM, Anderson RR, Webb RH. In vivo confocal scanning microscopy of human skin II: Advances in instrumentation and comparison with histology. J Invest Dermatol. 1999; 113:293–303. [PubMed: 10469324]
29. Subramanian M, Koedam JA, Wagner DD. Divergent fates of P- and E-selectins after their expression on the plasma membrane. Mol Biol Cell. 1993; 4:791–801. [PubMed: 7694691]

30. Kuijpers TW, Raleigh M, Kavanagh T, Janssen H, Calafat J, Roos D, Harlan JM. Cytokine-activated endothelial cells internalize E-selectin into a lysosomal compartment of vesiculotubular shape: A tubulin driven process. J Immunol. 1994; 152:5060–5069. [PubMed: 7513727]
31. Everts Kok RJ, Asgeirsdottir SA, Melgert BN, Moolenaar TJM, Koning GA, van Luyn MJA, Meijer DKF, Molema G. Selective intracellular delivery of dexamethasone into activated endothelial cells, using an E-selectin-directed immunoconjugate. J Immunol. 2002; 168:883–889. [PubMed: 11777986]
32. Muzykantov VR, Christofidou-Solomidou M, Balyasnikova I, Harshaw DW, Schultz L, Fisher AB, Albeda SM. Streptavidin facilitates internalization and pulmonary targeting of an anti-endothelial cell antibody (platelet-endothelial cell adhesion molecule 1): A strategy for vascular immunotargeting of drugs. Proc Natl Acad Sci USA. 1999; 96:2379–2384. [PubMed: 10051650]
33. Eppihimer MJ, Wolitsky B, Anderson DC, Labow MA, Granger DN. Heterogeneity of expression of E- and P-selectins in vivo. Circ Res. 1996; 79:560–569. [PubMed: 8781489]
34. Xu H, Forrester JV, Liversidge J, Crane IJ. Leukocyte trafficking in experimental autoimmune uveitis: Breakdown of blood-retinal barrier and upregulation of cellular adhesion molecules. Invest Ophthalmol Vis Sci. 2003; 44:226–234. [PubMed: 12506079]
35. Yeh DC, Bula DV, Miller JW, Gragoudas ES, Arroyo JG. Expression of leukocyte adhesion molecules in human subfoveal choroidal neovascular membranes treated with and without photodynamic therapy. Invest Ophthalmol Vis Sci. 2004; 45:2368–2373. [PubMed: 15223819]
36. Sipkins DA, Wei X, Wu JW, Runnels JM, Cote D, Means TK, Luster AD, Scadden DT, Lin CP. *In vivo* imaging of specialized bone marrow endothelial microdomains for tumor engraftment. Nature. 2005; 435:969–973. [PubMed: 15959517]
37. Luscinskas FW, Gimbrone MA Jr . Endothelial-dependent mechanisms in chronic inflammatory leukocyte recruitment. Ann Rev Med. 1996; 47:413–421. [PubMed: 8712792]
38. Smith ML, Olson TS, Ley K. CXCR2- and E-Selectin-induced neutrophil arrest during inflammation in vivo. J Exp Med. 2004; 200:935–939. [PubMed: 15466624]
39. Sipkins DA, Cheresh DA, Kazemi MR, Nevin LM, Bednarski MD, Li KC. Detection of tumor angiogenesis in vivo by alphaVbeta3-targeted magnetic resonance imaging. Nat Med. 1998; 4:623–626. [PubMed: 9585240]
40. Winter PM, Caruthers SD, Kassner A, Harris TD, Chinen LK, Allen JS, Lacy EK, Zhang H, Robertson JD, Wickline SA, Lanza GM. Molecular imaging of angiogenesis in nascent Vx-2 rabbit tumors using a novel alpha(nu)beta3-targeted nanoparticle and 1.5 Tesla magnetic resonance imaging. Cancer Res. 2003; 63:5838–5843. [PubMed: 14522907]
41. Dilanthra B, Ellegala HL-P, Carpenter JE, Klibanov AL, Kaul S, Shaffrey ME, Sklenar J, Lindner JR. Imaging tumor angiogenesis with contrast ultrasound and microbubbles targeted to $\alpha_v\beta_3$. Circulation. 2003; 108:336–341. [PubMed: 12835208]
42. Eppihimer MJ, Russell J, Anderson DC, Epstein CJ, Laroux S, Granger DN. Modulation of P-selectin expression in the postischemic intestinal microvasculature. Am J Physiol Gastroint Liver Physiol. 1997; 273:G1326–G1332.
43. Wei X, Runnels JM, Lin CP. Indocyanine green labels reticulocytes in circulation. Invest Ophthalmol Vis Sci. 2003; 44:4489–4496. [PubMed: 14507897]
44. Chong BF, Murphy JE, Kupper TS, Fuhlbrigge RC. E-selectin, thymus- and activation-regulated chemokine/CCL17, and intercellular adhesion molecule-1 are constitutively coexpressed in dermal microvessels: A foundation for a cutaneous immunosurveillance system. J Immunol. 2004; 172:1575–1581. [PubMed: 14734737]
45. Pober JS, Kluger MS, Schechner JS. Human endothelial cell presentation of antigen and the homing of memory/effector T cells to skin. Ann NY Acad Sci. 2001; 941:12–25. [PubMed: 11594565]
46. Nakada MT, Amin K, Christofidou-Solomidou M, O'Brien CD, Sun J, Gurubhagavatula I, Heavner GA, Taylor AH, Paddock C, Sun Q-H, Zehnder JL, Newman PJ, Albeda SM, DeLisser HM. Antibodies against the first Ig-like domain of human platelet endothelial cell adhesion molecule-1 (PECAM-1) that inhibit PECAM-1-dependent homophilic adhesion block in vivo neutrophil recruitment. J Immunol. 2000; 164:452–462. [PubMed: 10605042]

47. Austrup F, Vestweber D, Borges E, Lohning M, Brauer R, Herz U, Renz H, Hallmann R, Scheffold A, Radbruch A, Hamann A. P- and E-selectin mediate recruitment of T-helper-1 but not T-helper-2 cells into inflammed tissues. Nature. 1997; 385:81–83. [PubMed: 8985251]

48. Rossiter H, Alon R, Kupper TS. T Selectins, T-cell rolling and inflammation. Mol Med Today. 1997; 3:214–222. [PubMed: 9176884]

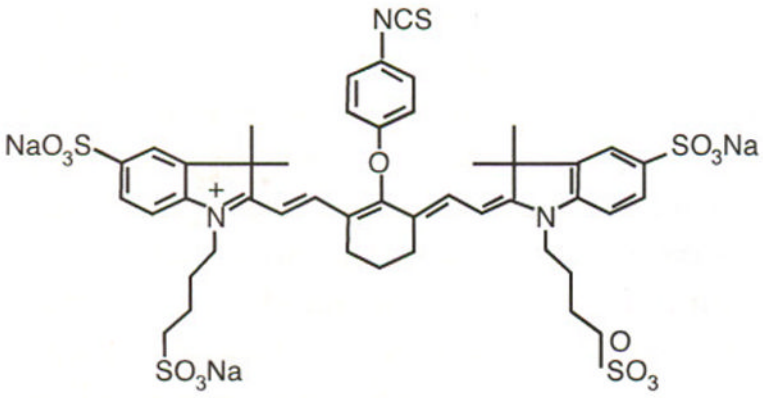

Figure 1.
Chemical structure of IRDye 38.

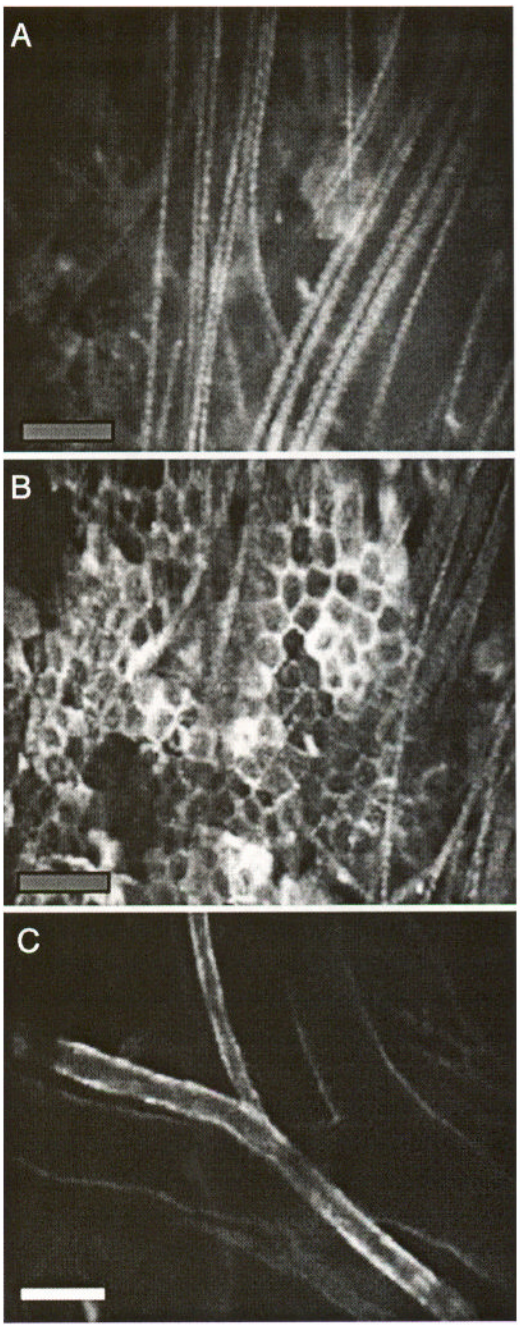

Figure 2.
Optical sectioning by in vivo confocal microscopy. (A) Autofluorescent surface hair, (B) autofluorescent epidermal keratinocytes, and (C) an artery and vein pair in a plane deeper than the keratinocyte layer. The vessels are stained with Cy5.5-conjugated anti-PECAM-1 antibody that had been intravenously injected 16 hr before the images were taken. Bars indicate 100 μm.

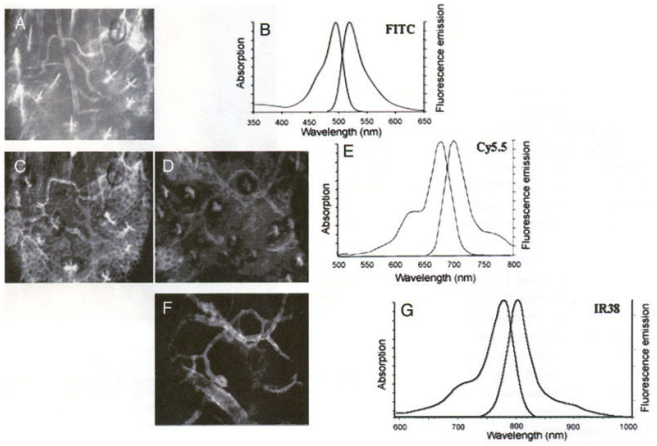

Figure 3.

Skin autofluorescence decreases at longer near-IR wavelengths. The tissue autofluorescence is most obvious in the FITC channel (A) compared to the Cy5.5 channel (C, D), and least obvious in the IR38 channel (F). (B, E, and G) Absorption and emission spectra for FITC, Cy5.5, and IR38fluorophores, respectively (A) FITC-conjugated anti-PECAM-1, (C) Cy5.5-conjugated anti-E-selectin, (D) Cy5.5-conjugated anti-E-selectin, and (F) IR38-conjugated anti-E-selectin with LPS treatment. Panels A and C are of the same site, as are panels D and F. The bowtie-like structures in A, C, and D are hair follicles. The honeycombed structures in A, C, and D are keratinocytes.

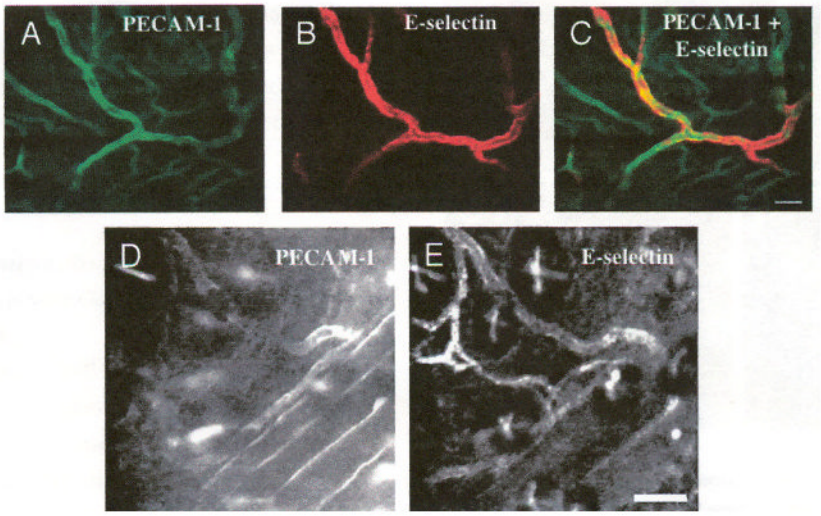

Figure 4.
Coexpression of constitutive E-selectin with PECAM-1. (A–E) Cy5.5-conjugated anti-E-selectin was injected into the tail vein followed by FITC-conjugated anti-PECAM-1 injection 2 days later. On the third day, the ear skin was imaged. (B, E) E-selectin is constitutively expressed in a subset of vessels expressing (A, D) PECAM-1. (C) Overlay of A and B. Images A–C from one mouse, D, E from a second mouse. Bars indicate 100 μm.

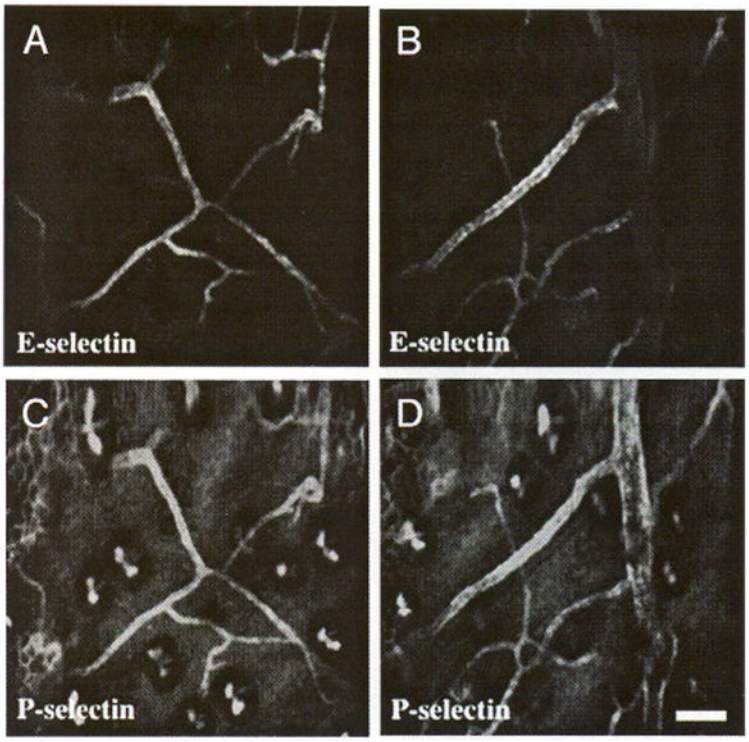

Figure 5.
Coexpression of E- and P-selectin in quiescent mouse skin. IR38-conjugated anti-E-selectin and Cy5.5-conjugaled anti-P-selectin were intravenously coinjected. Two days later, the vasculature in the mouse ear was imaged. (A, B) Expression of E-selectin is restricted to small venules, whereas (C, D) P-selectin is expressed in those venules as well as larger venules. Images A and C, and B and D are of the same sites, respectively. Bar indicates 100 μm.

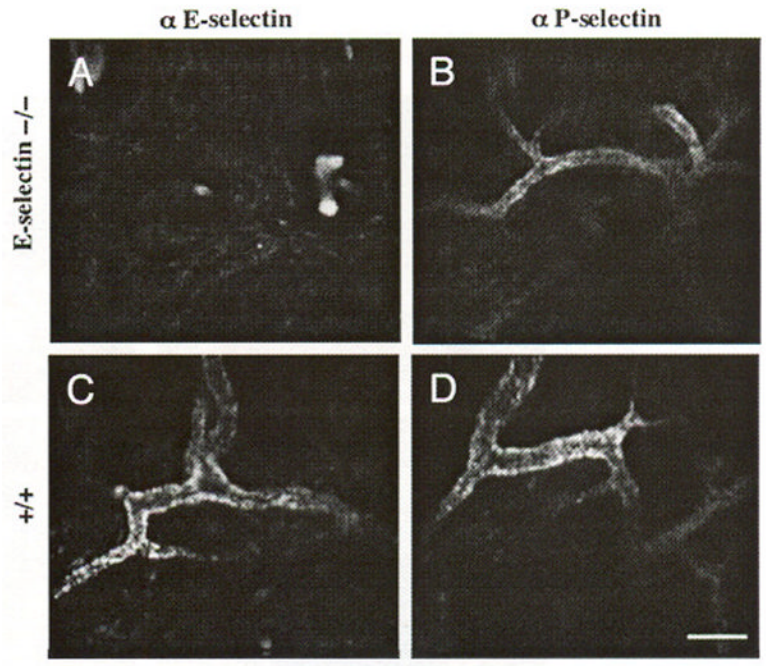

Figure 6.

Specificity of Cy5.5 conjugated E- and P-selectin antibodies in vivo is demonstrated in the skin of Balb/c E-selectin knockout mice. (B) A characteristic quiescent P-selectin expression pattern is present in E-selectin knockout mouse skin, but no E-selectin (A) expression is detected. Both (C) E-selectin and (D) P-selectin are expressed on skin vessel walls in the control mice in the quiescent state. Each panel represents a separate animal. Bar indicates 50 μm.

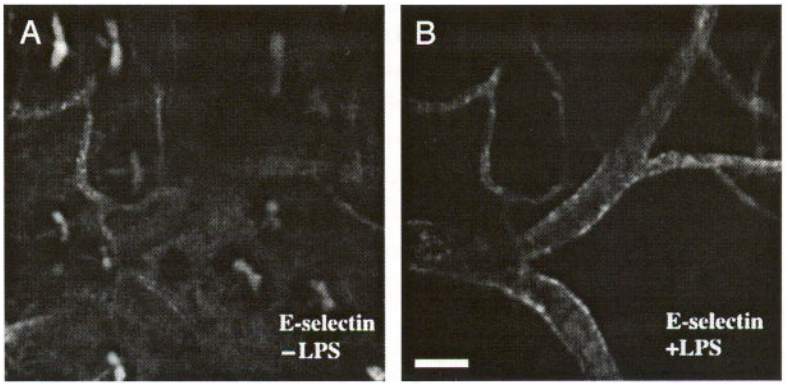

Figure 7.

LPS induces E-selectin expression in venules larger than 50 μm. Intravenous injection of Cy5.5-conjugated anti-E-selectin antibody was followed by intravenous injection of IR38-conjugated anti-E-selectin and intraperitoneal injection of LPS 9 days later. On Day 12. the mouse was imaged. E-selectin is constitutively expressed in postcapillary venules in (A) skin, but is expressed on larger venules after LPS induction (B). Images A and B are of the same site in the mouse ear skin. Bar indicates 100 μm.

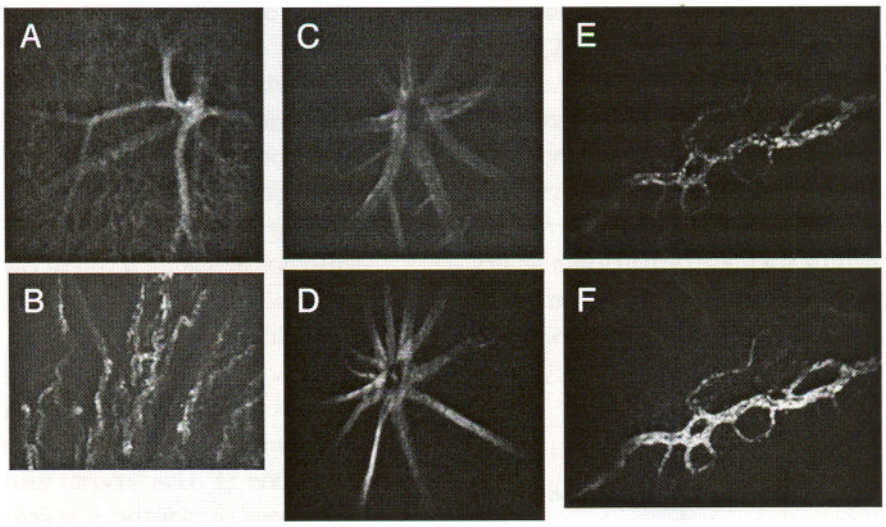

Figure 8.

In vivo fluorescence confocal microscopy can be performed on ocular tissues. PECAM-1 expression in the retina (A) and choroid (B) of a mouse 24 hr after intravenous injection of Cy5.5-conjugated anti-PECAM antibody. Cy5.5-conjugated anti-VCAM in a normal C57BL/6 mouse (C) and in a LPS-treated mouse retina (D). Cy5.5-conjugated anti-E-selectin in the conjunctiva of a normal mouse (E) and IR38-conjugated anti-E-selectin 24 hr after systemic administration of LPS (F).